Paleoceanography and Paleoclimatology

RESEARCH ARTICLE
10.1029/2024PA005071

Timing of Pedogenic Carbonate Formation in Fine-Grained Soils: Decoupled $T(\Delta_{47})$ and $\delta^{18}O_w$ Seasonal Bias

Rachel Havranek[1], Kathryn Snell[1], Sarah Brookins[1], and Brett Davidheiser-Kroll[2]

[1]Geological Sciences, University of Colorado Boulder, Boulder, CO, USA, [2]Thermo Fisher Scientific (Bremen) GmbH, Bremen, Germany

Key Points:

- This work provides further evidence that fine-grained soils will often have a different seasonal bias than coarse-grained soils
- In fine-grained, carbonate bearing soils there is very little annual-scale variation in the isotopic composition of soil water at depths >50 cm
- We infer that the difference in seasonal bias is due to slower dry-down in fine-grained soils, delaying pedogenic carbonate formation into the fall

Supporting Information:

Supporting Information may be found in the online version of this article.

Correspondence to:

R. Havranek,
Rachel.havranek@utah.edu

Citation:

Havranek, R., Snell, K., Brookins, S., & Davidheiser-Kroll, B. (2025). Timing of pedogenic carbonate formation in fine-grained soils: Decoupled $T(\Delta_{47})$ and $\delta^{18}O_w$ seasonal bias. *Paleoceanography and Paleoclimatology*, *40*, e2024PA005071. https://doi.org/10.1029/2024PA005071

Received 21 NOV 2024
Accepted 4 FEB 2025

Author Contributions:

Conceptualization: Rachel Havranek, Kathryn Snell, Brett Davidheiser-Kroll
Data curation: Rachel Havranek, Kathryn Snell, Brett Davidheiser-Kroll
Formal analysis: Rachel Havranek, Kathryn Snell
Funding acquisition: Rachel Havranek, Kathryn Snell
Investigation: Rachel Havranek, Kathryn Snell, Sarah Brookins
Methodology: Rachel Havranek, Kathryn Snell, Brett Davidheiser-Kroll
Project administration: Rachel Havranek, Kathryn Snell
Supervision: Kathryn Snell, Brett Davidheiser-Kroll
Validation: Rachel Havranek
Visualization: Rachel Havranek, Sarah Brookins
Writing – original draft: Rachel Havranek

Abstract Historically, clumped isotope thermometry ($T(\Delta_{47})$) of soil carbonates has been interpreted to represent a warm-season soil temperature based dominantly on coarse-grained soils. Additionally, $T(\Delta_{47})$ allows the calculation of the oxygen isotope composition of soil water ($\delta^{18}O_w$) in the past using the temperature-dependent fractionation factor between soil water and pedogenic carbonate, but previous work has not measured $\delta^{18}O_w$ values with which to compare to these archives. Here, we present clumped isotope thermometry of modern soil carbonates from three soils in Colorado and Nebraska, USA, that have a fine-to-medium grain size, contain clay, and are representative of many carbonate-bearing paleosols preserved in the rock record. At two of the three sites, Briggsdale, CO and Seibert, CO, $T(\Delta_{47})$ overlaps with mean annual soil temperature (MAST), and the calculated $\delta^{18}O_w$ overlaps within uncertainty with measured $\delta^{18}O_w$ at carbonate bearing depths. At the third site, in Oglala National Grassland, NE, mean $T(\Delta_{47})$ is 8–11°C warmer than MAST, and the calculated $\delta^{18}O_w$ has a significantly higher isotope value than any observations of $\delta^{18}O_w$. At all three sites, even in the fall season, $\delta^{18}O_w$ values at carbonate bearing depths overlap with spring rainfall $\delta^{18}O_w$, and there is little to no evaporative enrichment of $\delta^{2}H_w$ and $\delta^{18}O_w$ values. These data challenge long-held assumptions that all pedogenic carbonate records a warm-season bias, and that $\delta^{18}O_w$ at carbonate-bearing depths is affected by evaporative enrichment.

Plain Language Summary The stable isotope composition of pedogenic carbonate nodules is used to reconstruct environmental parameters like hydrology, vegetation, soil temperature, and atmospheric CO_2 from the geologic record. However, our understanding about how and when pedogenic carbonate nodules form mostly comes from modern coarse-grained soils, even though many climate records from the geologic past come from fine-grained paleosols. In this study, we examined three fine-grained, clay-bearing soils in the western Great Plains. We compared numerous environmental parameters (e.g., soil temperature, air temperature, etc.) and the stable isotope composition of soil water with temperatures and water isotope values calculated from carbonate clumped isotope thermometry. Our data are consistent with carbonate formation in the fall; the temperatures we measured directly from the soil during the fall match those of our isotopic thermometer. Interestingly, one soil did not match this behavior, and may suggest more complicated formation dynamics at play. Our soil water isotope data suggest that carbonate records information about precipitation at the time of greatest infiltration (e.g., spring), which may not match the season that temperature is recorded. This work is important because it challenges the long-held assumptions about pedogenic clumped isotope thermometry, and provides nuance about how paleoclimate records should be interpreted.

1. Introduction

Pedogenic carbonate nodules are a commonly used material for paleoenvironment reconstructions, because multiple stable isotope measurements (e.g., $\delta^{13}C$, $\delta^{18}O$, Δ_{47}, $\Delta^{17}O$, etc.) can be used as proxy measurements for many environmental conditions of interest, such as vegetation composition (Cerling, 1984; Cerling & Quade, 1993; Passey, 2012), ancient pCO_2 (e.g., Breecker et al., 2010; Da et al., 2019; Ji et al., 2018; Zhang et al., 2018), changes in the hydrologic system (Kelson et al., 2023; Levin et al., 2011; Passey, 2012; Passey et al., 2014), and temperature change associated with both climatic changes and tectonic evolution (e.g., Carrapa et al., 2014; DeCelles et al., 2007; Garzione et al., 2006; Ghosh et al., 2006; Huntington & Lechler, 2015; Ingalls et al., 2018; Rugenstein & Chamberlain, 2018; Snell et al., 2013). To improve our understanding of the relationship between the stable isotope compositions of pedogenic carbonates and environmental conditions in the geologic past, the geoscience community has studied 'modern' carbonate formation in Holocene soils, which serve as an approximation of modern conditions (e.g., Breecker et al., 2009; Burgener et al., 2016; Cerling, 1984;

Writing – review & editing:
Rachel Havranek, Kathryn Snell, Sarah Brookins, Brett Davidheiser-Kroll

Cerling & Quade, 1993; Hough et al., 2014; Huth et al., 2019; Kelson et al., 2020; Peters et al., 2013). These modern calibration studies are useful for constraining the strengths and limitations of pedogenic carbonate as a proxy for paleoenvironmental conditions.

Most modern calibration studies on pedogenic carbonate done over the last 10–15 years have capitalized on the development of clumped isotope thermometry to both understand the relationship between a clumped isotope temperature ($T(\Delta_{47})$) and air temperature and to improve our understanding of the timing and mechanism of pedogenic carbonate formation (Burgener et al., 2016; Gallagher & Sheldon, 2016; Hough et al., 2014; Hudson et al., 2024; Huth et al., 2019; Peters et al., 2013). An additional benefit of clumped isotope measurements is that it is possible to calculate the isotopic composition of the soil water that the carbonate precipitated from, which offers additional insight into formation mechanism, timing and soil hydrology processes. However, few studies to date have made use of the additional potential insight from the $\delta^{18}O$ of soil water ($\delta^{18}O_w$). In modern calibration studies, soils have generally been chosen as part of climatic or elevation gradients and have broadly been conducted in immature, medium to coarse grained soils (Burgener et al., 2018; Hough et al., 2014; Huth et al., 2019; Oerter & Amundson, 2016; Peters et al., 2013). In a synthesis of these studies, soil grain size appears to be an important control on the temperature (i.e., mean annual temperature vs. warm-season biased temperature) that was recorded by pedogenic carbonate, with coarser grained soils more biased toward warmer temperatures (Gallagher & Sheldon, 2016; Kelson et al., 2020). This synthesis also demonstrated that there was limited data from fine-grained and clay-rich soils as compared to other grain size classes. The observation of a grain-size influenced temperature bias, alongside the limited amount of temperature and soil water isotope data from fine grained and clay-rich soils, is important because many terrestrial paleoclimate records are based on pedogenic carbonate datasets from fine-grained and clay-rich paleosols (e.g., Bowen et al., 2015; Da et al., 2019; Driese et al., 2016; Salazar-Jaramillo et al., 2022). While the geologic community clearly understands the sets of processes that influence carbonate mineral formation, it is unclear which (if any) dominate pedogenic carbonate mineral formation, and how these are affected by (or vary with) soil texture.

To fill the critical gap in our understanding of carbonate formation in fine grained and clay-rich soils, we studied three Holocene fine-to-medium grained, clay-containing soils in Colorado and Nebraska, USA. We used clumped isotope thermometry, climatological data and soil data to learn about carbonate formation in these soils. Additionally, in this study, we include measurements of precipitation, regional surface water and soil water stable isotope geochemistry to gain a deeper understanding of how the oxygen isotope composition of carbonate records information about the hydrologic cycle.

2. Background

2.1. Stable Isotope Geochemistry of Pedogenic Carbonate

The $\delta^{18}O$ value of pedogenic carbonate ($\delta^{18}O_C$) is a function of both the temperature at which the mineral formed and the $\delta^{18}O_w$ from which the mineral precipitated (e.g., Cerling, 1984; Kim & O'Neil, 1997). The $\delta^{18}O_w$ value is initially set by the $\delta^{18}O$ value of meteoric water, but can be modified by evaporation (e.g., Cerling & Quade, 1993; Hough et al., 2014; Quade et al., 2007); the extent to which evaporation modifies the recorded $\delta^{18}O_c$ value is unknown at most sites (e.g., Breecker et al., 2009).

$T(\Delta_{47})$ provides an estimate of pedogenic carbonate formation temperature through a relationship between temperature and the degree of bond ordering of the heavy, rare isotopes ^{13}C and ^{18}O (Eiler, 2007). At low temperatures there is a greater degree of ^{13}C - ^{18}O ordering, or clumping, in the carbonate ion (CO_3^{2-}) compared to a purely random, stochastic distribution of the rare heavy isotopes, leading to an inverse relationship between Δ_{47} and temperature (Eiler, 2007). $T(\Delta_{47})$ can additionally be used with the simultaneously measured $\delta^{18}O_C$ to estimate the $\delta^{18}O_w$ that the carbonate formed from, using an equation for the temperature-dependent fractionation of oxygen isotopes between carbonate minerals and water (e.g., Daëron et al., 2019; Kim & O'Neil, 1997).

2.2. Pedogenic Carbonate Formation

There are three primary levers that control carbonate mineral formation in soils. First, pCO_2 of the soil environment, which is controlled by primary productivity and soil permeability, acts as a control on soil water pH; carbonate mineral formation is favored at lower soil pCO_2 (e.g., Breecker, 2013; Cerling & Quade, 1993). Second, soil temperature controls carbonate mineral formation because CO_2 becomes less soluble in water as

temperatures increase, and therefore carbonate solids are favored to form at higher temperatures. Soil temperature is controlled by the surface temperature and the thermal properties of the soil which is influenced by texture, porosity, water content, bulk density, and mineralogy (e.g., de Vries, 1952; Hillel, 2004). Lastly, increased calcium availability can drive mineral formation. Calcium cation availability depends on the delivery of calcium either from the soil substrate and/or from detrital material, both of which are influenced by local geology and water movement through the soil column (e.g., Birkeland, 1999; Zamanian et al., 2016). Under drying soil conditions, Ca^{2+} can become increasingly concentrated, driving supersaturation (e.g., Breecker et al., 2009; Hough et al., 2014). Over the last 40 years, there has been considerable effort to understand which of these levers dominates pedogenic carbonate formation and controls the timing and style of pedogenic carbonate formation, in part to improve interpretation of paleoenvironmental proxies (Breecker et al., 2009; Burgener et al., 2018; Cerling, 1984; Cerling & Quade, 1993; Hough et al., 2014; Huth et al., 2019; Kelson et al., 2020; Oerter & Amundson, 2016; Peters et al., 2013). Recent work also suggests that the timing and relative magnitude of carbonate mineral dissolution strongly influences the preserved isotope record (Breecker et al., 2025; Huth et al., 2019).

In general, there are three approaches that fall along a continuum that have been used to study pedogenic carbonate formation in Holocene soils. The first approach is to create a timeseries of the $\delta^{13}C$ value of soil CO_2 alongside timeseries of relevant soil conditions, including soil temperature, soil moisture, and/or soil pCO_2 (e.g., Breecker et al., 2009; Oerter & Amundson, 2016). These studies either measure $\delta^{18}O_w$ once to establish equilibrium, or assume equilibrium between $\delta^{18}O$ of CO_2 and the $\delta^{18}O_w$ to interpret the timing of carbonate formation. Then, theoretical $\delta^{13}C_C$ and $\delta^{18}O_C$ are calculated from the timeseries data, and are compared to the measured $\delta^{13}C_C$ and $\delta^{18}O_C$ of pedogenic carbonate. The second approach omits measurements of the $\delta^{13}C$ value of soil CO_2, and instead adds carbonate clumped isotope data. These studies create a time series of environmental parameters, such as soil temperature, soil moisture, air temperature, precipitation amounts, and $\delta^{18}O$ value of precipitation ($\delta^{18}O_p$). Then clumped isotope data ($T(\Delta_{47})$, $\delta^{13}C_C$, $\delta^{18}O_C$, and calculated $\delta^{18}O_w$) are used to constrain the timing of pedogenic carbonate formation from the same, or nearby sites (Burgener et al., 2016, 2018; Hough et al., 2014; Peters et al., 2013). The final approach, taken by Huth and others (2019), was to add soil water isotopes taken from discrete samples a few times throughout the study to the second approach, thereby circumventing assumptions of isotopic equilibrium. While all of these studies display nuance related to their particular field sites, the current consensus is that at low to moderate elevations (<4000 m), across a broad range of environmental conditions, pedogenic carbonate clumped isotope temperatures are typically biased towards warm season temperatures, and the dominant hypothesis is that soil dry-down drives pedogenic carbonate formation (Breecker et al., 2009; Burgener et al., 2016, 2018; Hough et al., 2014; Huth et al., 2019; Kelson et al., 2020; Oerter & Amundson, 2016; Peters et al., 2013). However, the majority of the studies highlighted above were conducted in poorly developed (e.g., inceptisol, entisol, aridisol), medium to coarse-grained soils. Soil texture is a primary control on the rate and style of soil dry-down because in a coarse-grained soil, the pores will empty quickly and become nonconductive even at high suction, whereas in a fine-grained soil the pores will empty more slowly and conductivity will not decrease as quickly even as suction increases (Hillel, 2004). Therefore, it makes sense that there may be a grain size bias in recorded clumped isotope temperatures (Kelson et al., 2020). This highlights a critical gap for paleoclimate studies that apply $T(\Delta_{47})$ fine-grained or clay-rich paleosols.

In addition, despite the importance for understanding both carbonate formation and interpreting the $\delta^{18}O_w$ archive, few of the above-mentioned studies characterize $\delta^{18}O_w$, which highlights an additional critical data gap. In a synthesis of the studies that incorporate clumped isotope thermometry data, the calculated mean $\delta^{18}O_w$ of all the datasets together was not biased towards summer precipitation values, as one might expect with the assumption that carbonate typically forms in the summer, but was instead similar to an integrated mean annual $\delta^{18}O_p$ value (Kelson et al., 2020). However, individual datasets within the compilation showed considerable scatter about the mean, and in some cases, a coherency that resulted in individual dataset means differing significantly from mean annual precipitation values. This result leaves open the question about how to interpret soil water $\delta^{18}O_w$ values derived from clumped isotope studies.

3. Methods

The general approach of this study was to compare pedogenic carbonate formation across three different soil textures within the same soil moisture regime (Ustic). From north to south, the three field sites are located in

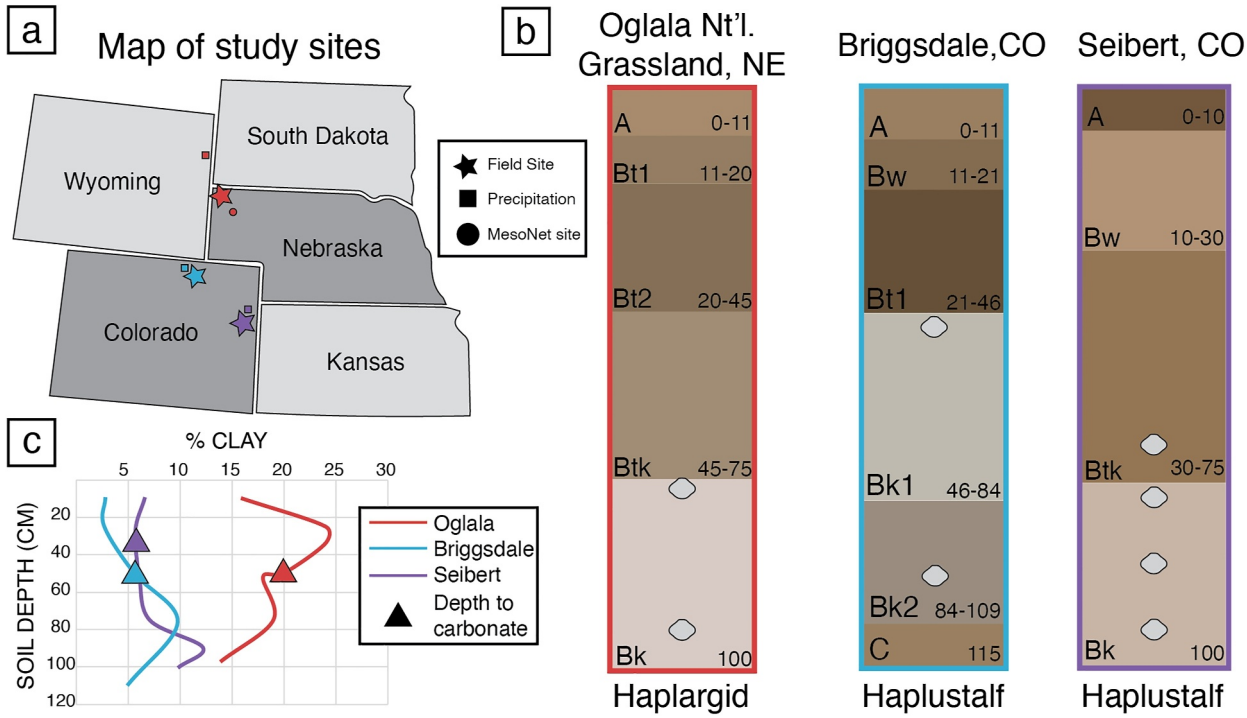

Figure 1. (a) Map of field site locations. From north to south, the field sites, noted with a star, are Oglala National Grassland (ONG, red), Briggsdale (blue), and Seibert (purple). The small squares are precipitation data collected by the National Ecological Observatory Network. The small red circle is the location of the Alliance MesoNet site. (b) Soil profiles of each site. Horizon depths, in cm, are noted at the bottom of each horizon. Note, the bottom depth is the depth of the described soil pit, not the base of the lowest horizon. The levels from which carbonate nodules were collected are shown as light gray spheroids. (c) The amount of clay (size fraction) as a function of depth. The triangle on each curve is the depth to carbonate.

Oglala National Grassland, NE (ONG, Latitude: 42.96 N°, Longitude: −103.56 E° (WGS 84), Elevation: 1,117 m)); Briggsdale, CO (Latitude: 40.59 N°, Longitude −104.32 E° (WGS 84), Elevation: 1,480 m); and, Seibert, CO (Latitude: 39.12 N°/Longitude: −102.93 E° (WGS 84), Elevation: 1,479 m) (Figure 1).

3.1. Field Methods

3.1.1. Meteorological Data From Oglala National Grassland, NE

The ONG site was instrumented with air temperature, relative humidity and precipitation quantity sensors in June 2021 (Onset, S-THC-M002 and Davis Instruments Rain gauge sensor, S-RGE-M002) (Figure 2b). However, due to significant livestock interference, this dataset is discontinuous. Therefore, we also incorporate data from the Alliance, Nebraska MesoNet site (Latitude: 42.18°N/Longitude: 102.92°E/Elevation: 1,241 m) that is 103 km to the southeast of the ONG site. The Nebraska MesoNet is supported by the state of Nebraska and operated by the University of Nebraska Lincoln. At the Alliance Mesonet site, air temperature, relative humidity, and precipitation quantity are recorded on an hourly basis, as well as soil moisture and temperature at 10, 25, 50, and 100 cm that are recorded at 1-minute intervals.

3.1.2. Meteorological Data From Briggsdale, CO and Seibert, CO

Both field sites in Colorado are co-located with CoAgMET sites, which are operated by the Colorado Climate Center, 2022 (Colorado State University, Fort Collins, CO). At both sites, the Colorado Climate Center measures air temperature, relative humidity, wind speed and direction, precipitation quantity, and soil temperature at 5 and 15 cm depths (Figure 2a). The Briggsdale site has been instrumented as a CoAgMET site since 31 July 2002 and the Seibert site has been instrumented since 2 April 2015.

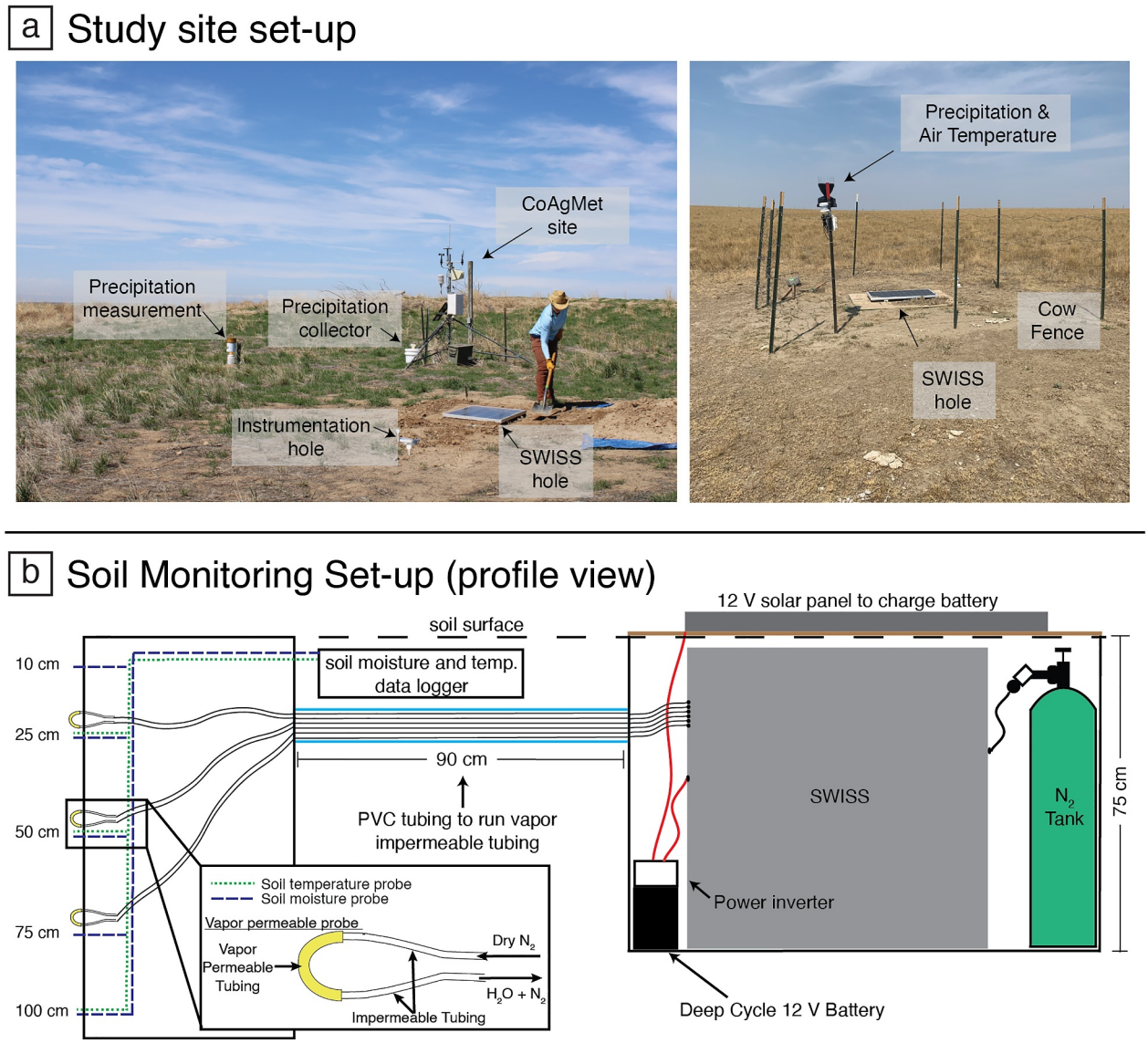

Figure 2. (a) Left, the field set-up at the Briggsdale site. The Seibert site is set up nearly identically to Briggsdale. The photo on the right shows the field set up at the ONG site. Key features of each site are labeled. (b) A profile view of the setup at each site. On the left is the instrumented hole where the soil temperature and moisture loggers as well as the vapor permeable probes were installed. On the right is the hole where the SWISS and power components were stored. Vapor impermeable tubing that connects the vapor permeable probes with the SWISS was buried at a depth of approx. 15 cm in a PVC pipe.

3.1.3. Soil Conditions

At each site, we excavated two holes (Figure 2b). We dug out the first hole once at the beginning of the study to install soil temperature and moisture loggers as well as water vapor sampling probes. We report soil temperature data at 25, 50, and 100 cm soil depth, and soil moisture at depths of 10, 25, 50, 75, and 100 cm. We also have soil temperature data from 10 to 75 cm from some sites, but to stay consistent in the comparison across sites, we excluded them. The excluded data do not affect any interpretations. We installed water vapor sampling probes into the intact sidewall of the pit at soil depths of 25, 50 and 75 cm. After logger and probe installation, we carefully backfilled the first hole with soil from approximately the same depths, taking care to compact the soil appropriately and maintain horizon depths as much as possible. We also excavated the second hole at the start of the study, and we maintained this hole throughout the study to store the soil water isotope storage system (SWISS) and associated components. We chose to store the SWISS units and associated components belowground to limit temperature variability experienced by the units, better protect against precipitation, weather, and animal

interference, and to make the sites more discreet to avoid human interference. Lastly, we connected the SWISS to the water vapor sampling probes via Bev-A-Line impermeable tubing, which was run through a PVC pipe buried at approximately 15 cm depth. Burying the impermeable tubing reduces the effect of diurnal temperature variability, and limits condensation as water vapor travels from the soil to the SWISS.

3.2. Soil Characterization

We excavated soil pits to a depth of 100 cm for soil description and sample collection. We collected bulk soil samples for soil texture and mineralogical analyses at depths of approximately 10, 25, 50, 75 and 100 cm. In some cases, we collected additional bulk soil samples from horizons or transitions of interest. For example, we collected extra samples where the character (size and/or hardness) of the pedogenic carbonate nodules changed or where there was a large change in soil color without a change in carbonate characteristics. At this time, we also collected pedogenic carbonate nodules for isotope geochemistry from at least two levels in each pit (Figure 1b).

Soil texture and mineralogical analyses were performed in the Sediment/Plant Analysis and Processing Lab and XRD/Soil Processing Lab, respectively, which are both in the Institute of Arctic and Alpine Research (INSTAAR) at the University of Colorado Boulder. We measured soil particle size using a Malvern Mastersizer 3000. Broadly, we defined soils that were <50% sand as fine-to medium-grained. For the purposes of this study, we define silt loam as fine-grained, sandy-loam as medium-grained and loamy sand as moderately coarse-grained. We characterized soil mineralogy using Siemens D5000 XRD with ROCKJOCK6 processing software. See Supporting Information S1 for greater detail.

3.3. Carbonate Nodule Characterization

Using thin sections of individual carbonate nodules, we used optical and cathodoluminescence (CL) microscopy to identify fabrics and textures consistent with primary carbonate formation as well possible additional, later stages of carbonate formation within the nodules. See Supporting Information S1 for greater detail.

To determine the approximate age of carbonate nodule formation, whole nodules from 2 to 3 soil levels from each site were dated using ^{14}C radiocarbon dating. Samples were prepared in the INSTAAR Laboratory for AMS Radiocarbon Preparation and Research. See Supporting Information S1 for greater detail.

3.4. Carbonate Stable Isotope Geochemistry

To produce sample powder for stable isotope geochemistry, we either (1) drilled nodules mounted in epoxy from which paired thin section were cut, or (2) crushed whole nodules and homogenized the powder using mortar and pestle.

We collected carbonate clumped isotope data during six sessions in 2022 and 2024 on a Thermo Scientific 253 Plus dual-inlet isotope ratio mass spectrometer with an on-line, custom-made vacuum extraction line in the University of Colorado Boulder Earth System Stable Isotope Laboratory (CUBES-SIL; RRID SCR-019300, Fetrow et al., 2022). The calcium carbonate standards ETH 1, 2, and 3 were used to correct the data to the community accepted Intercarb-Carbon Dioxide Equilibrium Scale (ICDES) (Bernasconi et al., 2021). In addition, when available in a given session the additional standards ETH-4, IAEA-C1, IAEA-C2 were added. The carbonate standard IAEA-C2 was used as a monitoring standard as it is a low-temperature standard with similar $\delta^{13}C_c$ and $\delta^{18}O_c$ values to our samples. Two samples from Briggsdale (B50 and B110) required a double-clean or bleach-clean protocol during measurement to sufficiently remove isobaric contaminants from the sample gas in order to determine a reliable $T(\Delta_{47})$ value (see Supporting Information S1). Prior to double cleaning, both samples yielded unreasonably cold temperatures (approx. −45°C), which can happen when there is contamination of mass-47 with non-CO_2 compounds. Additionally, to test if the high temperatures from the ONG site were due to contamination effects, we treated 3 additional samples. After an initial replicate of each of those samples, the Δ_{47} values from the ONG were not significantly from other values from that site, so we did not pursue further replicates.

Temperatures were estimated from the mean Δ_{47} values using the Anderson et al. (2021) calibration line, and temperature uncertainties were estimated by propagating the Δ_{47} standard error for every sample (Daëron, 2020). See Supporting Information S1 for greater detail. From the measured $T(\Delta_{47})$ and $\delta^{18}O_c$ values, we calculated the $\delta^{18}O_w$ value that the carbonate mineral precipitated from using the equilibrium fractionation between calcite and

water established by Daëron et al. (2019). The $\delta^{18}O_w$ value are reported as the per mil (‰) deviation relative to VSMOW/SLAP (Coplen, 2011). Repeatability of all Δ_{47} (anchors + unknowns) was 0.0183‰.

3.5. Water Stable Isotope Geochemistry

3.5.1. Precipitation and Surface Water Stable Isotope Geochemistry

We collected integrated monthly precipitation samples for stable isotope analysis ($\delta^{18}O_p$ and δ^2H_p) following Scholl et al. (1996). We measured the precipitation in the INSTAAR Stable Isotope Laboratory at CU Boulder using a Picarro L2130-*i* Isotope and Gas Concentration Analyzer paired with an autosampler and high precision vapourizer unit. We measured 2–3 replicates of each sample. The isotope values were corrected for instrument drift during the run period and memory effects between samples, and $\delta^{18}O_p$ and δ^2H of precipitation (δ^2H_p) values are reported as the per mil (‰) deviation relative to VSMOW/SLAP. Final sample $\delta^{18}O_p$ and δ^2H_p values were calculated as the mean value of replicates; error is reported as 2 sigma standard deviation. Precision varied by run, but for $\delta^{18}O$ was between 0.02 and 0.03‰, and for δ2H was between 0.09 and 0.14‰.

To complement precipitation isotope data from the study sites, we also collated precipitation isotope data from nearby National Ecological Observation Network (NEON) sites that are relatively proximal to both field sites in Colorado (Water Isotopes Database, 2017). There was no existing proximal precipitation isotope data available in the Nebraska panhandle region, and so we instead use data from the US Network of Isotopes in Precipitation (US NIP) site located in Newcastle, WY (Water Isotopes Database, 2017).

3.5.2. Soil Water Isotope Geochemistry

We collected two soil water isotope time series from all three field sites using Soil Water Isotope Storage System (SWISS) units (Havranek et al., 2020, 2023). The SWISS units are capable of autonomously collecting 15 soil water vapor samples in the field over a ∼1 month interval (and longer in some cases) before returning the units back to the laboratory for stable isotope analysis (Havranek et al., 2023). As noted in Section 3.1.3, water vapor probes for vapor collection were installed at depths of 25, 50 and 75 cm at all three field sites. We collected soil water vapor samples at intervals of 5–7 days; the SWISS was under development during this interval, and so while the units were deployed continuously from June 2021 to September 2021 and April 2022 to October 2022, only two ∼1 month soil water isotope time series from 2022 yielded reliable data for each site. Maximum storage time for all SWISS units was 41 days.

We measured soil water vapor samples in the INSTAAR Stable Isotope Laboratory using a continuous flow Picarro L2130-*i* Isotope and Gas Concentration Analyzer. We measured samples using the dry-air carrier gas method to enhance measurement stability; see Supporting Information S1 for greater detail (Havranek et al., 2023). Water vapor sample values were converted to liquid water values using a correction specific to the vapor permeable membrane tubing (Rothfuss et al., 2013). We then corrected for isotope scale compression, and report all $\delta^{18}O_w$ and δ^2H of soil water (δ^2H_w) values as the per mil (‰) deviation relative to VSMOW/SLAP. Finally, an offset correction of 1.0 and 2.6‰ for $\delta^{18}O_w$ and δ^2H_w, respectively, associated with the storage and measurement of water vapor via the SWISS, was applied (Havranek et al., 2023). For all soil water samples, we report an uncertainty of 0.9 and 3.5‰ for $\delta^{18}O_w$ and δ^2H_w, respectively. Both the offset correction and assessment of uncertainty are based on a series of experiments in which water vapor of known composition was introduced into the SWISS units, stored for 14 days, and then measured (Havranek et al., 2023).

4. Results

4.1. Meteorological Data

For each site below, we focus on changes in soil conditions at a depth of 50 cm, because for two of the three sites pedogenic carbonate nodules are first observed near that depth. Further, many paleosol carbonates are collected roughly from this depth (30–50 cm) because of considerations about atmospheric CO_2, radiative heating of the soil surface, evaporative enrichment of oxygen isotopes, and so on.

In Alliance, NE, soil temperature varies sinusoidally throughout the year, and at 50 cm depth, soil temperature peaks in August (Figure 3a). At the ONG site, soil moisture varied sinusoidally through the year at depths ≥50 cm,

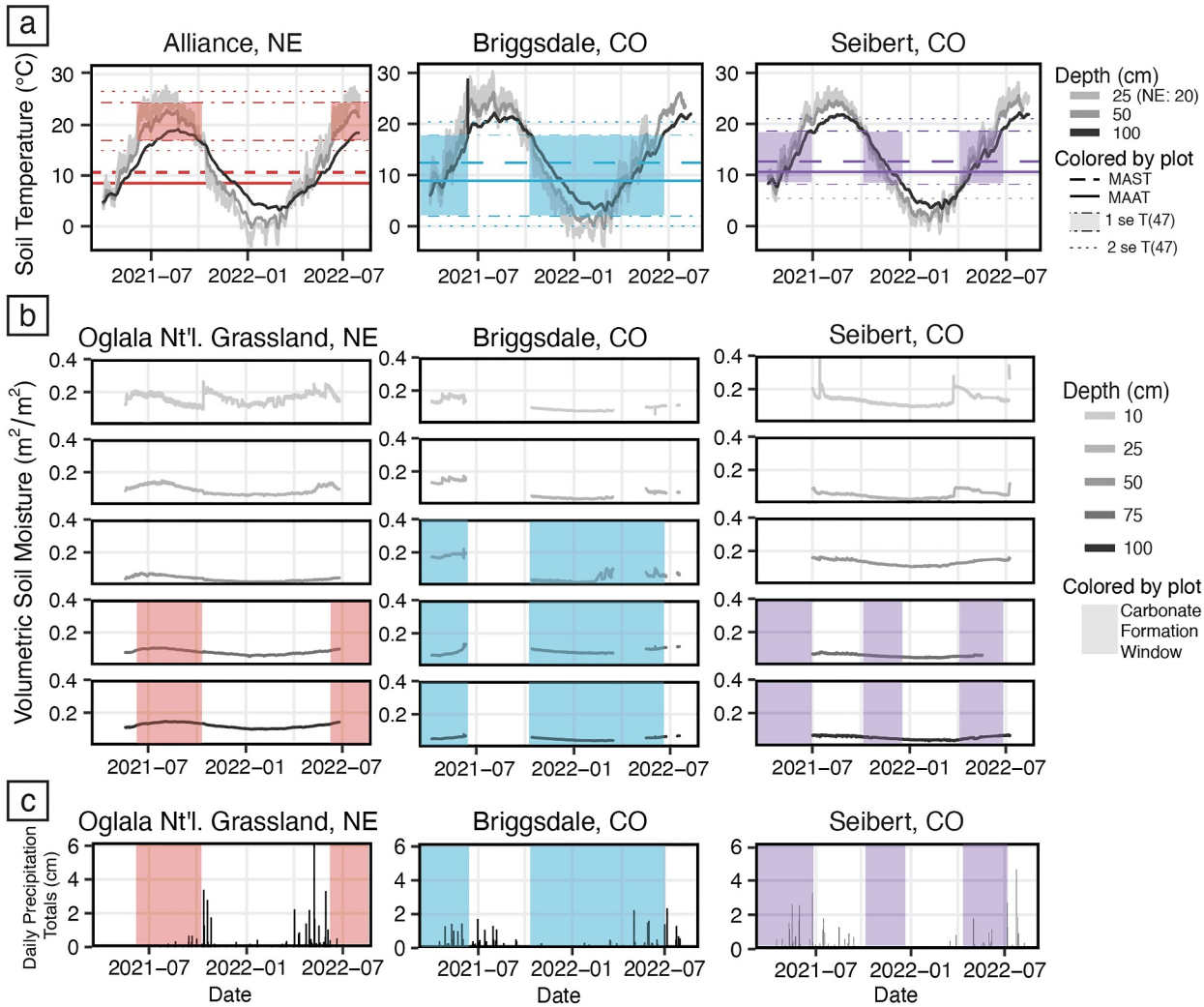

Figure 3. (a) Soil temperature from May 2021 to August 2022 for all three field sites. The translucent boxes highlight soil temperatures that overlap within uncertainty of all clumped isotope temperatures of carbonate nodules from that site (uncertainty inclusive). The dashed line is the mean annual soil temperature (MAST) at 50 cm depth, and the solid line is the mean annual air temperature (MAAT). (b) Soil moisture from May 2021 to August 2022. Translucent boxes highlight the same time periods highlighted in (a) Only soil depths where carbonate nodules form are highlighted. (c) Daily precipitation totals for each site. Translucent boxes highlight the same time periods as in (a).

and was not responsive to intense rain events like soil moisture at depths of 10 and 25 cm. Precipitation is summer biased, with peak precipitation amounts in June (Figure S1a in Supporting Information S1).

Soil temperature varies sinusoidally at the Briggsdale site and maximum soil temperatures at 50 cm depth are reached in August (Figure 3a). Volumetric soil moisture at a depth of 50 cm varied widely from December 2020 to October 2022 between 0.05 and 0.22 m^3/m^3 (Figure 3b). Precipitation at this site is summer biased, and is typically highest in May (Figure S1b in Supporting Information S1). At the Seibert site, soil temperature varies sinusoidally and at 50 cm depth, peaks in August (Figure 3a). At soil depths of 25 cm and below, soil moisture varies sinusoidally (Figure 3b), while at a depth of 10 cm, soil moisture is responsive to snow melt and rain fall events (Figure 3b). Precipitation dominantly falls in the summer months, with the most precipitation in May and July (Figure S1c in Supporting Information S1).

4.2. Soil and Carbonate Nodule Characterization

The soil at the ONG site has a silt loam texture (fine-grained) (Figure S2 in Supporting Information S1), and has an argillic horizon, where there is an accumulation of smectite clays. The presence of smectitic clays allows for

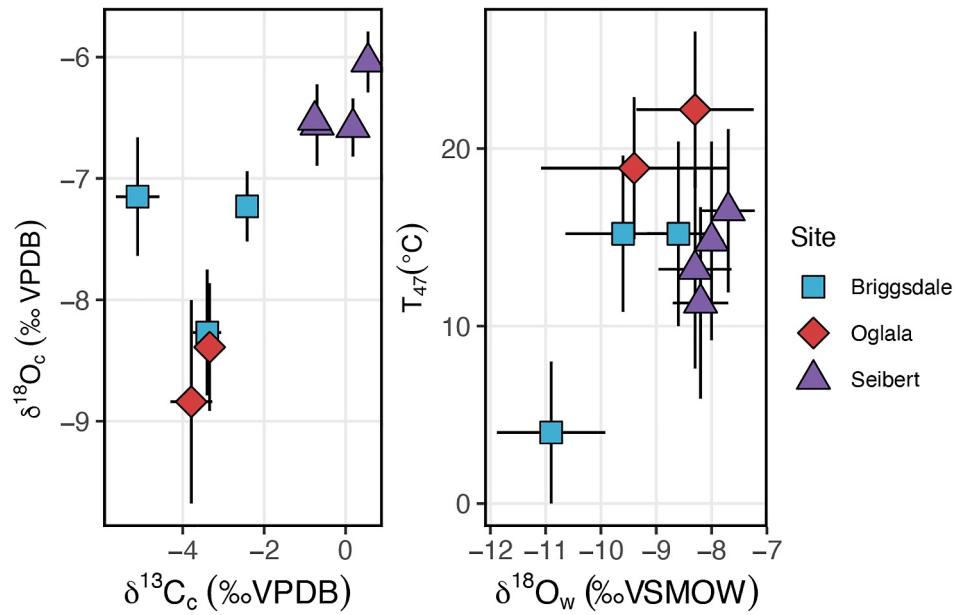

Figure 4. Stable isotope results. (a) $\delta^{13}C_c$ versus. $\delta^{18}O_c$. (b) $T(\Delta_{47})$ versus calculated $\delta^{18}O_w$. In both plots, error is plotted as 2 standard error.

cracking that, in the dry season, extends to the surface of the soil. In the argillic horizon, soil peds displayed small slickensides, consistent with shrink-swell behaviors associated with the presence of smectite clays. The clay size fraction reaches a maximum in the Bt2 horizon, at 24% (Figure 1c), and carbonate formation in this soil begins below the Bt2 horizon. Depth to carbonate formation at this site is 52 cm, with the presence of nodules starting at 75 cm, and the carbonate bearing horizon continues to the bottom of the described pit. Two nodules from the ONG site that were collected at depths of 75 and 100 cm yield ^{14}C dates of 7,220 ± 20 and 8,765 ± 25 radiocarbon years BP, respectively.

The upper portion of the soil profile at the Briggsdale site (<45 cm depth) has a loamy sand (moderately coarse-grained) texture and the lower portion of the soil profile has a sandy loam (medium-grained) texture (Figure S2 in Supporting Information S1). Clay particle size fraction in the soil profile slowly increases throughout the profile, and the clay size fraction reaches a maximum in the Bk horizon, at 9.8% (Figure 1c). Depth to carbonate formation is 50 cm, and nodule formation begins at the same level. Two carbonate nodules from the Briggsdale site that were collected at depths of 64 and 84 cm yield ^{14}C dates of 6,980 ± 20 and 8,200 ± 25 radiocarbon years BP, respectively.

The uppermost 30 cm of the soil at the Seibert site has a sandy loam (medium-grained) texture, and below 30 cm has a silty loam (fine-grained) texture (Figure S2 in Supporting Information S1). The clay size fraction reaches a maximum of 12% in the Bk horizon, at a depth of 90 cm (Figure 1c). The depth to carbonate formation is the shallowest of the three sites at 30 cm but between 30 and 75 cm carbonate is extremely diffuse and is not present as discrete masses. Carbonate nodule formation starts at a depth of approximately 75 cm. The carbonate nodules at this site also have a slightly different morphology than the other sites - they incorporate large fragments (>250 μm length) of other minerals like feldspar and quartz (Figures S4 and S5 in Supporting Information S1). Two carbonate nodules from the Seibert site collected at depths of 75 and 100 cm depth yield ^{14}C dates of 9,680 ± 30 and 7,655 ± 25 radiocarbon years BP, respectively.

Across all three sites, carbonate was typically non-luminescent to dully luminescent under CL (Figure S4 in Supporting Information S1). In the nodules from the ONG site, there were brightly luminescent clasts that had the mottling and shape of earthworm calcite granules (Prud'homme et al., 2018). All of the nodules were multi-mineralic and included clasts of quartz, feldspars and clays (Figure S5 in Supporting Information S1).

Carbonate nodule stable isotope results are presented in Figure 4 and Table 1. In general, $\delta^{13}C_c$ and $\delta^{18}O_c$ are positively correlated, and grouped by field site. Clumped isotope temperatures for all three sites generally cluster

Table 1
Stable Isotope Data From Modern Pedogenic Carbonate Nodules at All Three Field Sites

Site	Sample (depth, cm)	N	$\delta^{13}C_c$ (‰ VPBD)	$\delta^{13}C_c$ 2sd (‰ VPBD)	$\delta^{18}O_c$ (‰ VPBD)	$\delta^{18}O_c$ 2sd (‰ VPBD)	Δ_{47} ICDES	Δ_{47}se ICDES	$T(\Delta_{47})$[a] (°C)	$T(\Delta_{47})$ 2se (°C)	$\delta^{18}Ow$[b] (‰ VSMOW)
Briggsdale	B105 (105 cm)	8	−5.11	0.53	−7.15	0.49	0.663	0.0077	4	4	−10.9
Briggsdale	B110[c] (110)	4	−3.40	0.35	−8.27	0.52	0.6243	0.0086	15.2	4.4	−9.6
Briggsdale	B50[d] (50)	3	−2.42	0.05	−7.23	0.29	0.6243	0.011	15.2	5.2	−8.6
Oglala	O75 (75)	8	−3.79	0.51	−8.84	0.84	0.6125	0.0072	18.9	4	−9.4
Oglala	O95 (95)	7	−3.34	0.35	−8.39	0.53	0.6023	0.008	22.2	4.4	−8.3
Seibert	S100 (100)	3	−0.7	0.11	−6.56	0.33	0.6309	0.0123	13.2	5.6	−8.3
Seibert	S75-80 (75–80)	3	0.55	0.05	−6.04	0.25	0.6373	0.0123	11.3	5.4	−8.2
Seibert	S80-85 (80–85)	5	0.18	0.06	−6.58	0.24	0.6202	0.0095	16.5	4.6	−7.7
Seibert	S90-95 (90–95)	3	−0.76	0.11	−6.52	0.11	0.6257	0.0122	14.8	5.6	−8

[a]Calculated using Anderson et al. (2021), $\Delta_{47} = 0.0391 \pm 0.0004 \times 10^6/T^2 + 0.154 \pm 0.004$. [b]Calculated using Daëron et al. (2019). [c]Indicates sample that was treated (Fiebig et al., 2024). [d]Indicates sample that was double-cleaned (See Text S1 for details).

between 11.3 ± 2.7°C and 22.2 ± 2.2°C, except for one nodule from Briggsdale which yielded a temperature of 4.0 ± 2.0°C.

4.3. Water Isotope Geochemistry

For all three sites, the integrated monthly precipitation isotope samples fall within the population of nearby precipitation or stream water samples (Figure S6, Table S2 in Supporting Information S1). In general, at all three sites, soil water from depths of 50 and 75 cm depth cluster together, and there is very little change in isotope value from summer (June-July) into the fall (September to October) (Figure 5). At the Briggsdale site, the soil water data from 50 to 75 cm depths in July 2022 fall above the global meteoric water line, while soil water isotope values from September 2022 fall below the global meteoric water line (Figure S6 in Supporting Information S1). At both the ONG and Seibert sites, soil water isotope values from 50 to 75 cm depth overlap with the local and global meteoric water lines. For all three sites, soil water isotope values from 25 cm in the fall months were offset to higher values.

5. Discussion

First, we discuss the assumptions associated with measuring modern environmental parameters and comparing those to pedogenic carbonate nodules that likely formed during the Holocene Climatic Optimum. Second, we discuss our confidence in the soil water isotope data. Then, we integrate all of the environmental and isotopic data and discuss the implications these data have for pedogenic carbonate formation mechanisms, and how that can and should inform future paleoclimate work.

5.1. Holocene Climate

One common challenge for modern calibration studies is that we are comparing instrumental data cover the last 1–10 years, while soil carbonates record conditions over 100–1,000 years. We, therefore, briefly explore how and if the climatic differences over the interval that the soil carbonate formed are meaningfully different than our modern observations. The ^{14}C dates from the carbonate nodules from all three sites yielded dates between 6,980 ± 20 and 9,680 ± 30 years before present. These dates are consistent with carbonate nodule formation during the Holocene Climatic Optimum, which persisted from ~9 Ka to– ~5Ka (Shuman & Marsicek, 2016; Steig, 1999).

In North America, temperatures during the Holocene Climatic Optimum were 0–1°C warmer than pre-industrial conditions, similar to today (IPCC, 2022; Shuman & Marsicek, 2016). Given the relatively small shift in temperatures relative to the current precision of the clumped isotope data (approx. ±3–5°C), the modern soil temperature structure is likely an appropriate approximation of soil temperature conditions at the time of carbonate formation.

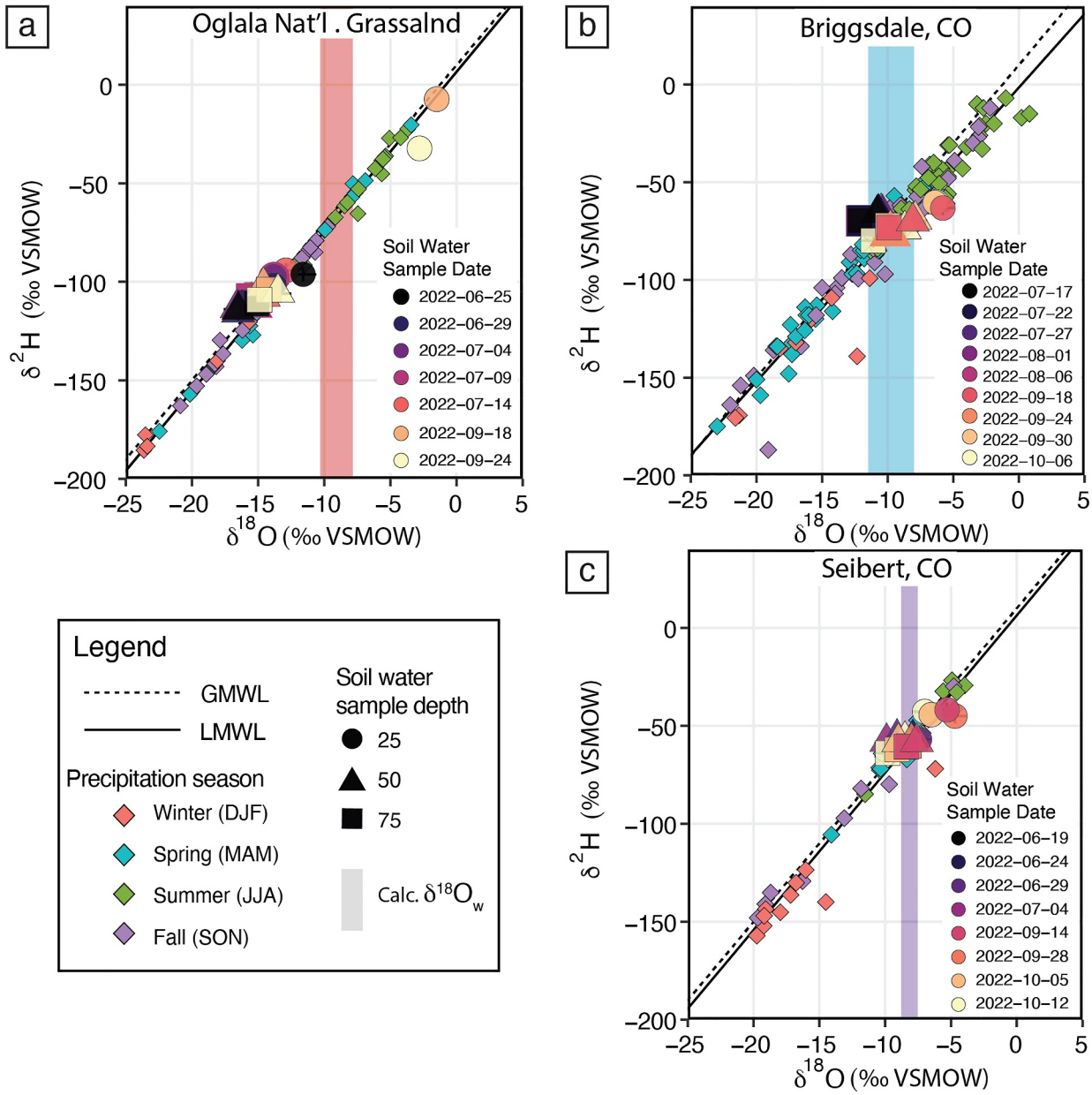

Figure 5. Soil water and precipitation isotope data for (a) ONG, (b) Briggsdale and (c) Seibert. The colored vertical bar in each plot is the calculated $\delta^{18}O_w$ from the carbonate clumped isotope data, 2 standard error uncertainty inclusive. Colors of the vertical bar match Figure 3.

Precipitation decreased in the mid-latitudes in North America during this time, likely as a consequence of a northward shift of westerly storm tracks (Routson et al., 2019; Shuman & Serravezza, 2017). Despite the drying, the $\delta^{18}O_p$ likely only varied by ~0.5‰ (Liu et al., 2014). Given the magnitude of uncertainty on our modern soil water oxygen isotope values (±1.0‰), and the soil water oxygen isotope values calculated from a clumped isotope measurement (approx. ±0.6‰), modern observations of soil moisture patterns, especially the magnitude of soil water isotope change at carbonate bearing soil depths, is likely a reasonable approximation of soil water during the time of carbonate formation.

Lastly, one significant challenge about the Briggsdale site is that the land use history of the site over the last 150 years is not well known. The American dustbowl of the 1930s strongly affected this portion of northeastern Colorado, and in this region, generally, the topsoil was over-tilled and often stripped away, which could explain

the absence of the mollic epipedon at the site. So, it is possible that the upper horizons at this site have been altered within the last 100 years.

5.2. Modern Soil Water Isotope Data

At ONG, soil water $\delta^{18}O_w$ and δ^2H_w values largely cluster together, except for two 25 cm depth samples in September 2022; those data are offset to significantly higher $\delta^{18}O_w$ and δ^2H_w values (Figure 5a). The water vapor concentrations for those two samples were also considerably lower than other samples (i.e., <15,000 ppm), coinciding with a time when the volumetric water content (VWC) of the soil fell below 0.1 m^3/m^3. The significantly higher uncertainty and non-linearity of isotope value measurements made below 10,000 ppm on Picarro L2130-I instruments could account for these high values, or they could reflect highly evaporated water related to the dry conditions. We cannot determine which is the case, however, the shallower depth of these samples relative to the carbonate bearing depths means the uncertainty of these values has little impact on our interpretations of the carbonate data. In contrast, the $\delta^{18}O_w$ and δ^2H_w values at carbonate bearing depths (50 and 75 cm) fall within error of the GMWL and do not show significant variability between June and September 2022. This is consistent with other observations of limited soil water isotope variability at depths 50 cm and greater (Oerter & Bowen, 2019; Quade et al., 2018). The annual average value of $\delta^{18}O_p$ from Newcastle, WY (110 km from the ONG site) is −11.2‰, and our soil water isotope values from 50 to 75 cm show a slight winter bias that is similar to regional groundwater (Jasechko et al., 2014). There is one potential meteorological explanation for this bias; soil water isotope monitoring was done during a La Niña event. It is challenging to know how different the soil water isotopes are year to year, but based on soil moisture data from the Alliance, NE mesonet site, it is likely that the soil was drier than previous years, with less summer precipitation.

Soil water isotope data at Briggsdale extends July–October 2022 (Figure 5b). There are several complexities to this soil water isotope dataset. First, all stable isotope values from 25 cm depth are more uncertain because water vapor concentrations were below 15,000 ppm during measurement due to low soil moisture (<0.1 m^3/m^3 VWC). Despite having similar $\delta^{18}O_w$ values, the samples collected in July 2022 from depths of 50 and 75 cm have δ^2H_w values that are 10–15‰ higher than for soil water samples collected in September-October; as a result, the samples from July to August fall above the GMWL. Previous work has shown that the $\delta^{18}O_w$ values and δ^2H_w values from SWISS measurements can be decoupled (Havranek et al., 2023). We hypothesize that this decoupling is a result of pressure gradients inadvertently created by introducing dry air into the flasks during the measurement of gas samples that more easily bias hydrogen isotope results (Steen-Larsen & Zannoni, 2024). We therefore interpret the oxygen isotope values from all dates at this site with greater confidence than the δ^2H_w. The calculated $\delta^{18}O_w$ value from the clumped isotope measurements (Figure 5b) overlaps within uncertainty of the measured $\delta^{18}O$ values from 50 to 75 cm depth.

All of the soil water isotope data from Siebert had sufficiently high water concentrations for robust measurement, with the exception of the September-October 2022 soil water samples from 25 cm depth which had low VWC. Data from 50 to 75 cm depth are relatively invariant across the nearly 4-month timespan. Similarly to the other two sites, the soil water isotope values from this site cluster together, except for the 25 cm depth samples September–October 2022 with low LWC, which again have higher $\delta^{18}O_w$ and δ^2H_w values. As a result, data from 9/14/22 and 9/28/22 fall off the global meteoric water line. The return to the GMWL on 10/5/22 and 10/12/22 may be a product of the infiltration of precipitation from 9/30/22 and 10/4/22 at this site.

The overlap of the measured $\delta^{18}O_w$ with the GMWL and the observation of very little variation of $\delta^{18}O_w$ from summer into the fall at carbonate bearing depths from all three sites (Figure 5) is consistent with many observations from the ecohydrology literature. First, fine grained soils have higher dispersivity than coarse-grained soils, and so it is expected that at depths ≥50 cm, mobile and immobile pore water is very effectively homogenized (Kabeya et al., 2007; Sprenger, Leistert, et al., 2016; Sprenger, Seeger, et al., 2016). Second, one dimensional models of soil water isotopes predict very little temporal variability in soil water isotopes at depths >25 cm. The model predicts low temporal variability because as the thickness of the dry soil layer increases, the evaporation rate decreases as diffusional resistance increases (Barnes & Allison, 1983). Finally, recent advances in soil water isotope sampling strategies have enabled the creation of temporal records of $\delta^{18}O_w$ and δ^2H_w that also show very little variation in isotope values at depths of 50 and 75 cm (Oerter & Bowen, 2019; Seeger & Weiler, 2021). Given the lack of change in $\delta^{18}O_w$ across the summer–fall at carbonate bearing depths, changes in soil moisture at these depths must be driven by processes that produce minimal isotope effects such as hydraulic

redistribution, root water uptake, preferential flow, and hydrodynamic dispersion (Barnes & Allison, 1983; Hillel, 2004; La Follette et al., 2023; Orlowski et al., 2015; Sprenger, Leistert, et al., 2016).

5.3. Pedogenic Carbonate Formation

One reason to study the impact of grain size and clay content on soil carbonate formation is because dewatering proceeds quickly in coarse-grained soils, whereas, in fine-grained and clay-rich soils, dewatering proceeds at much slower rates (Gaur & Mohanty, 2016; Hillel, 2004). As a result, in fine-grained and clay-rich soils, soil dry-down continues later into the fall season in summer-dominated precipitation regimes. It is logical, therefore, that if soil dewatering is the primary driver of carbonate mineral supersaturation, there may be a grain-size bias in preserved clumped isotope temperatures (Kelson et al., 2020). Here, we examine the hypothesis of soil dewatering as the primary driver of carbonate supersaturation in fine-medium grained soils from two perspectives: T (Δ_{47}) and $\delta^{18}O_w$.

At the Briggsdale and Siebert sites, carbonate clumped isotope temperatures overlap with mean annual soil temperature (MAST) (Figure 3a). This result is consistent with other studies of fine to medium grained soils (Kelson et al., 2020). A temperature approximately equivalent to MAST points to net carbonate formation in either the fall or spring season. Carbonate formation in the spring would suggest that carbonate mineral formation is being driven primarily by Ca^{2+} ion delivery by an advective flux of water from the surface; carbonate formation in the fall would be more consistent with a combination of soil-dry down and a concomitant decrease in soil pCO_2 as the driving mechanisms of carbonate formation. At both the Briggsdale and Siebert sites, the calculated value of $\delta^{18}O_w$ from clumped isotope measurements overlaps within uncertainty of modern measurements of $\delta^{18}O_w$ (Figures 5b and 5c), and the lack of seasonal variability in $\delta^{18}O_w$ at carbonate bearing depths means that soil water isotopes on their own cannot be used to distinguish between either Ca^{2+} ion delivery or soil dewatering with decreasing pCO_2 as the driver of carbonate supersaturation. Geochemical modeling has demonstrated that infiltration commonly results in net dissolution, and so it is unlikely that net carbonate precipitation occurs during the spring (Huth et al., 2019). At Briggsdale, data gaps don't allow us to evaluate the style of dry-down at ≥50 cm depth in the fall. However, it is typical at these depths that soil moisture variability is somewhat sinusoidal. At Seibert, we observe a sinusoidal change in soil moisture, and the low variability in overall soil moisture at depths ≥50 cm (Figure 3b) signals that if dewatering is the ultimate driving mechanism in fine grained soils, then the degree of variation needed to reach super saturation is very small. Other studies have emphasized the role of soil CO_2 in driving pedogenic carbonate formation in arid soils (Breecker et al., 2009; Oerter & Amundson, 2016), as well as its role in conjunction with soil moisture (Huth et al., 2019), and so an important next avenue of research in these, and other fine grained soils, would be to simultaneously monitor soil pCO_2 at ≥50 cm (Huth et al., 2019) to constrain the magnitude of variability of that parameter.

In contrast to the other two sites, at the ONG site, clumped isotope temperatures are ∼10°C higher than MAST and overlap with soil temperatures at carbonate bearing depths between late-June and October (Figure 3a). The calculated $\delta^{18}O_w$ is similar in value to late spring - summer $\delta^{18}O_p$ (Figure 5a). At face value, the T(Δ_{47}) and $\delta^{18}O_c$ data together require that pedogenic carbonate formed during a period of peak soil temperatures either in equilibrium with summer precipitation or with evaporatively ^{18}O-enriched soil water. However, the calculated $\delta^{18}O_w$ is ∼6‰ higher than the measured $\delta^{18}O_w$ at carbonate bearing depths during the summer-fall (Figure 5a). Throughout the period of peak soil temperatures, the measured $\delta^{18}O_w$ at carbonate bearing depths (≥50 cm) is more similar to a winter (snow-melt) or early spring isotope value than a summer precipitation value (Figure 5a). Moreover, the soil moisture data do not indicate that there either is an infiltration pulse to depths ≥50 cm during the summer that would accommodate the delivery of isotopically heavier water, or enough evaporation to drive a 6‰ change in $\delta^{18}O_w$ (Figure 3b). The in situ soil water isotope data and soil moisture data, therefore require that we consider alternative carbonate formation mechanisms.

One potential hypothesis to explain the clumped isotope data from the ONG site is that cracking of the soil from the shrinking of 2:1 clays caused rapid soil CO_2 degassing, which in turn caused pedogenic carbonate to form out of isotopic equilibrium with the DIC pool, creating anomalously high T(Δ_{47}) and $\delta^{18}O_w$ (Affek & Zaarur, 2014; Tripati et al., 2015). There are two ways to test this hypothesis. The first is to do paired soil organic matter and pedogenic carbonate $\delta^{13}C$ analysis, which could indicate if pedogenic carbonate is forming in equilibrium under very high soil CO_2 (water-logged) conditions, or under low-productivity conditions (Montañez, 2013). The second way to test this hypothesis is with dual-clumped isotope thermometry (Bajnai et al., 2020; Fiebig

et al., 2021). This tool compares the temperature calculated from the mass-48 CO_2 isotopologue with the temperature generated simultaneously from mass-47 to assess if a $T(\Delta_{47})$ value reflects isotopic equilibrium (i.e., the Δ_{47} and Δ_{48} temperatures are the same) or is the result of kinetic processes such as rapid CO_2 degassing (Bajnai et al., 2020; Fiebig et al., 2021). There were two reasons we did not evaluate Δ_{48} in this study; first, the precision of the data in study are not high enough to evaluate Δ_{48}, and second, very small amounts of contamination can drive large variation in mass-48 (Fiebig et al., 2024), and this was of extra concern in modern soils near (<200 m) from active agricultural sites. A second potential explanation for the mismatch between the observed and calculated $\delta^{18}O_w$ is the sorption of atmospheric vapor to clay minerals during deep cracking, leading to disequilibrium between the total soil water pool and the liquid water that carbonate forms in equilibrium with. While our data don't allow us to rigorously evaluate this hypothesis, the influence of vapor sorption is minimal above gravimetric water contents greater than 10%, and at the time of measurement, volumetric water content at this site was between 8% and 14% (Oerter & Bowen, 2017). Overall, the high clumped isotope temperature and calculated $\delta^{18}O_w$ are challenging to explain without one of these mechanisms for disequilibrium and points to a need for future work at this site, and in other carbonate bearing clay-rich soils. Data from the ONG site indicate the need to include and consider soil water isotope datasets in future modern calibration efforts.

5.4. Implications for Paleoclimate Studies

One important implication of this study for the paleosol carbonate proxy is that this study substantiates previous findings that in fine grained and clay-rich soils, pedogenic carbonate clumped isotope temperatures can reflect mean annual air temperatures (Kelson et al., 2020). This calls into question previous attempts to estimate seasonality based on $T(\Delta_{47})$ of paleosol carbonates from fine-grained, clay-rich soils, as these studies assumed a warm season bias of carbonate formation in their seasonality estimates (e.g., Hyland et al., 2018; Snell et al., 2013). This work also highlights the utility of creating clumped isotope records of ancient examples of climate change (e.g., Paleocene-Eocene Thermal Maximum, middle Miocene Climatic Optimum, etc.) to understand phenomena such as polar amplification and terrestrial amplification of warming, because fine grained, clay rich soils may give us a view into mean change, not just seasonal change.

The second implication of this work is that in fine grained and clay-rich soils, at carbonate bearing depths, the $\delta^{18}O_w$ has a value that is set by the largest pulse of precipitation. In many parts of the western United States, the largest pulse of precipitation is often during the late spring from a combination of snow melt and larger spring season precipitation events. There is very little seasonal evolution of $\delta^{18}O_w$ at depths >50 cm after the value is initially set (Oerter & Bowen, 2019; Seeger & Weiler, 2021; Stern et al., 1999), and our data is consistent with these previous studies. Most paleoclimate studies using paleosol carbonates assumed that $T(\Delta_{47})$ and the calculated $\delta^{18}O_w$ have the same seasonal bias, but the lack of variation in measured $\delta^{18}O_w$ through the year leads to a decoupling between the season that $T(\Delta_{47})$ records (fall) and the precipitation season recorded (spring). These data support the need for thoughtful interrogation of the dominant precipitation season in the geologic past to interpret both $T(\Delta_{47})$ and the calculated $\delta^{18}O_w$, and consideration of the role of snowmelt in ancient soils under different climatic regimes (Hudson et al., 2024).

A final consideration regards the conventional wisdom over the last 30 years that the $\delta^{18}O_w$ calculated from paleosol carbonate $T(\Delta_{47})$ values are most often evaporatively ^{18}O-enriched relative to the precipitation that sourced the water. Another implication of this work is that pedogenic carbonate in fine grained and clay rich soils do not in fact record an evaporatively enriched signal in the calculated $\delta^{18}O_w$. This aligns with recent developments in and observations of triple oxygen isotopes on pedogenic carbonates that show the degree of evaporative enrichment in pedogenic carbonate is highly variable (Kelson et al., 2023). More modern calibration work is needed to understand what controls if and when carbonate records evaporatively enriched soil water so that $\delta^{18}O_w$ can be reliably used for paleoclimate and paleoaltimetry applications as well as to calibrate isotopically enabled global circulation models in the past and future (Campbell et al., 2024; Winnick et al., 2015). This conclusion also supports the hypothesis that we can also design experiments to exploit soil depth to target evaporative signals more deliberately (Kelson et al., 2023).

6. Conclusions

In this study, we present data on carbonate formation in three modern soils from Colorado and Nebraska, USA. These three soils span soil textures from loamy sand (medium grained) to silty loam (fine grained) with up to 24%

clay. To understand the timing of pedogenic carbonate formation in these soils, we compared modern observational environmental data, including observations of soil water isotopes and historical climate data from three mesonet sites, with pedogenic carbonate clumped isotope temperature and $\delta^{18}O_w$ data.

Clumped isotope temperatures from pedogenic carbonate overlap with MAST at both sites in Colorado, but clumped isotope temperatures are 8–11°C warmer than MAST at the most clay-rich field site in Nebraska. Similarly, the $\delta^{18}O_w$ calculated from the clumped isotope temperatures overlap within uncertainty of the measured $\delta^{18}O_w$ from carbonate bearing depths at both sites in Colorado. In contrast, at the Nebraska site, the calculated $\delta^{18}O_w$ is about 6‰ higher than observations of $\delta^{18}O_w$ at carbonate bearing depths. At all three sites, observed $\delta^{18}O_w$ was nearly invariant from summer-fall, and overlapped with spring $\delta^{18}O_p$. These data support the interpretation that, in most cases, in fine-grained, clay-rich soils it is appropriate to interpret pedogenic carbonate clumped isotope temperatures as representative of mean annual soil temperatures. The combination of soil water isotope data and clumped isotope data also demonstrate that, in fine-grained soils, pedogenic carbonate from ≥50 cm may record a $\delta^{18}O_w$ value that is set by the largest pulse of precipitation and has very little summer evaporative enrichment.

Data Availability Statement

All raw data as well as the R markdown files used for data processing can be found in the OSF repository (Havranek et al., 2025).

Acknowledgments
Funds for this project were provided by NSF grant EAR 2023385 and the University of Colorado Boulder to K. Snell. We thank CoAgMet which is operated by the Colorado Climate Center for site and data access, with special recognition for the families that allowed us access to CoAgMet sites located on private land. Access to Oglala National Grassland was granted through Special Use Permit PRD203. The authors thank the Nebraska Mesonet operated by the State of Nebraska in collaboration with the Department of Natural Resources and the Institute of Agriculture and Natural Resources at the University of Nebraska Lincoln for data access. We thank the entire INSTAAR Stable Isotope Lab both for instrument access as well as for invaluable discussions and assistance during this project. The authors would also like to thank Wendy Roth for assistance obtaining soil grain size and mineralogy data, and Dr. Scott Lehman for assistance with ^{14}C data. We had many field assistants for this work, but want to especially thank Spencer Burns, Anne Fetrow, Juliana Olsen-Valdez, and Haley Brumberger for their invaluable help. Lastly, the authors thank Julia Kelson and an anonymous reviewer for constructive reviews that greatly improved this manuscript. This study was done on the ancestral homelands of the Cheyenne, Arapahoe, Lakota, and Apache, and Ute peoples.

References

Affek, H. P., & Zaarur, S. (2014). Kinetic isotope effect in CO2 degassing: Insight from clumped and oxygen isotopes in laboratory precipitation experiments. *Geochimica et Cosmochimica Acta*, *143*, 319–330. https://doi.org/10.1016/j.gca.2014.08.005

Anderson, N. T., Kelson, J. R., Kele, S., Daëron, M., Bonifacie, M., Horita, J., et al. (2021). A unified clumped isotope thermometer calibration (0.5–1100°C) using carbonate-based standardization. *Geophysical Research Letters*, *48*(7), 1–11. https://doi.org/10.1029/2020gl092069

Bajnai, D., Guo, W., Spötl, C., Coplen, T. B., Methner, K., Löffler, N., et al. (2020). Dual clumped isotope thermometry resolves kinetic biases in carbonate formation temperatures. *Nature Communications*, *11*(1), 4005. https://doi.org/10.1038/s41467-020-17501-0

Barnes, C. J., & Allison, G. B. (1983). The distribution of deuterium and 18O in dry soils. 1. Theory. *Journal of Hydrology*, *60*(1–4), 141–156. https://doi.org/10.1016/0022-1694(83)90018-5

Bernasconi, S. M., Daëron, M., Bergmann, K. D., Bonifacie, M., Meckler, A. N., Affek, H. P., et al. (2021). InterCarb: A community effort to improve Interlaboratory standardization of the carbonate clumped isotope thermometer using carbonate standards. *Geochemistry, Geophysics, Geosystems*, *22*(5). https://doi.org/10.1029/2020GC009588

Birkeland, P. (1999). *Soils and geomorphology*. Oxford University Press.

Bowen, G. J., Maibauer, B. J., Kraus, M. J., Röhl, U., Westerhold, T., Steimke, A., et al. (2015). Two massive, rapid releases of carbon during the onset of the Palaeocene-Eocene thermal maximum. *Nature Geoscience*, *8*(1), 44–47. https://doi.org/10.1038/NGEO2316

Breecker, D. O. (2013). Quantifying and understanding the uncertainty of atmospheric CO2 concentrations determined from calcic paleosols. *Geochemistry, Geophysics, Geosystems*, *14*(8), 3210–3220. https://doi.org/10.1002/ggge.20189

Breecker, D. O., Michel, L. A., Rasmussen, C., & Tabor, N. J. (2025). A biogeochemical perspective on pedogenesis from soils to paleosols. In *Treatise on geochemistry* (pp. 353–409). Elsevier. https://doi.org/10.1016/B978-0-323-99762-1.00094-2

Breecker, D. O., Sharp, Z. D., & McFadden, L. D. (2009). Seasonal bias in the formation and stable isotopic composition of pedogenic carbonate in modern soils from central New Mexico, USA. *Bulletin of the Geological Society of America*, *121*(3–4), 630–640. https://doi.org/10.1130/B26413.1

Breecker, D. O., Sharp, Z. D., & McFadden, L. D. (2010). Atmospheric CO2 concentrations during ancient greenhouse climates were similar to those predicted for A.D. 2100. *Proceedings of the National Academy of Sciences of the United States of America*, *107*(2), 576–580. https://doi.org/10.1073/pnas.0902323106

Burgener, L. K., Huntington, K. W., Hoke, G. D., Schauer, A., Ringham, M. C., Latorre, C., & Díaz, F. P. (2016). Variations in soil carbonate formation and seasonal bias over >4 km of relief in the western Andes (30°S) revealed by clumped isotope thermometry. *Earth and Planetary Science Letters*, *441*, 188–199. https://doi.org/10.1016/j.epsl.2016.02.033

Burgener, L. K., Huntington, K. W., Sletten, R., Watkins, J. M., Quade, J., & Hallet, B. (2018). Clumped isotope constraints on equilibrium carbonate formation and kinetic isotope effects in freezing soils. *Geochimica et Cosmochimica Acta*, *235*, 402–430. https://doi.org/10.1016/j.gca.2018.06.006

Campbell, J., Poulsen, C. J., Zhu, J., Tierney, J. E., & Keeler, J. (2024). CO_2-driven and orbitally driven oxygen isotope variability in the Early Eocene. *Climate of the Past*, *20*(3), 495–522. https://doi.org/10.5194/cp-20-495-2024

Carrapa, B., Huntington, K. W., Clementz, M., Quade, J., Bywater-Reyes, S., Schoenbohm, L. M., & Canavan, R. R. (2014). Uplift of the Central Andes of NW Argentina associated with upper crustal shortening, revealed by multiproxy isotopic analyses. *Tectonics*, *33*(6), 1039–1054. https://doi.org/10.1002/2013TC003461

Cerling, T. E. (1984). The stable isotopic composition of modern soil carbonate and its relationship to climate. *Earth and Planetary Science Letters*, *71*(2), 229–240. https://doi.org/10.1016/0012-821x(84)90089-x

Cerling, T. E., & Quade, J. (1993). Stable carbon and oxygen isotopes in soil carbonates. *Geophysical Monograph Series*, *78*, 217–231. https://doi.org/10.1029/gm078p0217

Colorado Climate Center. (2022). CoAgMet [dataset]. Retrieved from http://www.coagmet.colostate.edu/

Coplen, T. B. (2011). Guidelines and recommended terms for expression of stable-isotope-ratio and gas-ratio measurement results. *Rapid Communications in Mass Spectrometry*, *25*(17), 2538–2560. https://doi.org/10.1002/rcm.5129

Da, J., Zhang, Y. G., Li, G., Meng, X., & Ji, J. (2019). Low CO2 levels of the entire Pleistocene epoch. *Nature Communications*, *10*(1), 4342. https://doi.org/10.1038/s41467-019-12357-5

Daëron, M. (2020). Full propagation of analytical uncertainties in D47 measurements. *Geochemistry, Geophysics, Geosystems*, *22*(1), 1–26. https://doi.org/10.1029/2020gc009592

Daëron, M., Drysdale, R. N., Peral, M., Huyghe, D., Blamart, D., Coplen, T. B., et al. (2019). Most Earth-surface calcites precipitate out of isotopic equilibrium. *Nature Communications*, *10*(1), 1–7. https://doi.org/10.1038/s41467-019-08336-5

DeCelles, P. G., Quade, J., Kapp, P., Fan, M., Dettman, D. L., & Ding, L. (2007). High and dry in central Tibet during the late Oligocene. *Earth and Planetary Science Letters*, *253*(3–4), 389–401. https://doi.org/10.1016/j.epsl.2006.11.001

De Vries, D. A. (1952). A nonstationary method for determining thermal conductivity of soil in situ. *Soil Science*, *73*(2), 83–90. https://doi.org/10.1097/00010694-195202000-00001

Driese, S., Peppe, D., Beverly, E., DiPietro, L., Arellano, L., & Lehmann, T. (2016). Paleosols and paleoenvironments of the early Miocene deposits near Karungu, lake Victoria, Kenya. *Palaeogeography, Palaeoclimatology, Palaeoecology*, *443*, 167–182. https://doi.org/10.1016/j.palaeo.2015.11.030

Eiler, J. M. (2007). "Clumped-isotope" geochemistry-The study of naturally-occurring, multiply-substituted isotopologues. *Earth and Planetary Science Letters*, *262*(3–4), 309–327. https://doi.org/10.1016/j.epsl.2007.08.020

Fetrow, A. C., Snell, K. E., Di Fiori, R. V., Long, S. P., & Bonde, J. W. (2022). How Hot is Too Hot? Disentangling mid-Cretaceous Hothouse paleoclimate from Diagenesis. *Paleoceanography and Paleoclimatology*, *37*(12), e2022PA004517. https://doi.org/10.1029/2022PA004517

Fiebig, J., Bernecker, M., Meijer, N., Methner, K., Staudigel, P. T., Davies, A. J., et al. (2024). Carbonate clumped isotope values compromised by nitrate-derived NO2 interferent. *Chemical Geology*, *670*, 122382. https://doi.org/10.1016/j.chemgeo.2024.122382

Fiebig, J., Daëron, M., Bernecker, M., Guo, W., Schneider, G., Boch, R., et al. (2021). Calibration of the dual clumped isotope thermometer for carbonates. *Geochimica et Cosmochimica Acta*, *312*, 235–256. https://doi.org/10.1016/j.gca.2021.07.012

Gallagher, T. M., & Sheldon, N. D. (2016). Combining soil water balance and clumped isotopes to understand the nature and timing of pedogenic carbonate formation. *Chemical Geology*, *435*, 79–91. https://doi.org/10.1016/j.chemgeo.2016.04.023

Garzione, C. N., Molnar, P., Libarkin, J. C., & MacFadden, B. J. (2006). Rapid late Miocene rise of the Bolivian Altiplano: Evidence for removal of mantle lithosphere. *Earth and Planetary Science Letters*, *241*(3–4), 543–556. https://doi.org/10.1016/j.epsl.2005.11.026

Gaur, N., & Mohanty, B. P. (2016). Land-surface controls on near-surface soil moisture dynamics: Traversing remote sensing footprints. *Water Resources Research*, *52*(8), 6365–6385. https://doi.org/10.1002/2015WR018095

Ghosh, P., Adkins, J., Affek, H. P., Balta, B., Guo, W., Schauble, E. A., et al. (2006). 13C-18O bonds in carbonate minerals: A new kind of paleothermometer. *Geochimica et Cosmochimica Acta*, *70*(6), 1439–1456. https://doi.org/10.1016/j.gca.2005.11.014

Havranek, R. E., Snell, K., Kopf, S., Davidheiser-Kroll, B., Morris, V., & Vaughn, B. (2023). Technical note: Lessons from and best practices for the deployment of the soil water isotope storage system. *Hydrology and Earth System Sciences*, *27*(15), 2951–2971. https://doi.org/10.5194/hess-27-2951-2023

Havranek, R. E., Snell, K. E., Davidheiser-Kroll, B., Bowen, G. J., & Vaughn, B. (2020). The Soil Water Isotope Storage System (SWISS): An integrated soil water vapor sampling and multiport storage system for stable isotope geochemistry. *Rapid Communications in Mass Spectrometry*, *34*(12), 1–11. https://doi.org/10.1002/rcm.8783

Havranek, R. E., Snell, K. E., Davidheiser-Kroll, B., & Brookins, S. (2025). Timing of pedogenic carbonate formation in fine-grained soils: Decoupled T(D47) and d18Ow seasonal bias. [Dataset]. *OSF*. https://doi.org/10.17605/OSF.IO/E7M35

Hillel, D. (2004). *Introduction to environmental soil physics*. Elsevier Academic Press.

Hough, B. G., Fan, M., & Passey, B. H. (2014). Calibration of the clumped isotope geothermometer in soil carbonate in Wyoming and Nebraska, USA: Implications for paleoelevation and paleoclimate reconstruction. *Earth and Planetary Science Letters*, *391*, 110–120. https://doi.org/10.1016/j.epsl.2014.01.008

Hudson, A. M., Kelson, J. R., Paces, J. B., Ruleman, C. A., Huntington, K. W., & Schauer, A. J. (2024). Clumped isotopes record a glacial-Interglacial shift in seasonality of soil carbonate accumulation in the san Luis valley, southern Rocky Mountains, USA. *Geochemistry, Geophysics, Geosystems*, *25*(4), e2023GC011221. https://doi.org/10.1029/2023GC011221

Huntington, K. W., & Lechler, A. R. (2015). Carbonate clumped isotope thermometry in continental tectonics. *Tectonophysics*, *647*, 1–20. https://doi.org/10.1016/j.tecto.2015.02.019

Huth, T. E., Cerling, T. E., Marchetti, D. W., Bowling, D. R., Ellwein, A. L., & Passey, B. H. (2019). Seasonal bias in soil carbonate formation and its implications for interpreting high-resolution paleoarchives: Evidence from southern Utah. *Journal of Geophysical Research: Biogeosciences*, *124*(3), 616–632. https://doi.org/10.1029/2018JG004496

Hyland, E. G., Huntington, K. W., Sheldon, N. D., & Reichgelt, T. (2018). Temperature seasonality in the North American continental interior during the early Eocene climatic optimum. https://doi.org/10.5194/cp-2018-28

Ingalls, M., Rowley, D., Olack, G. A., Currie, B., Li, S., Schmidt, J., et al. (2018). Paleocene to Pliocene low-latitude, high-elevation basins of southern Tibet: Implications for tectonic models of India-Asia collision, Cenozoic climate, and geochemical weathering. *Bulletin of the Geological Society of America*, *130*(1–2), 307–330. https://doi.org/10.1130/B31723.1

IPCC. (2022). *Global Warming of 1.5°C*. https://doi.org/10.1017/9781009157940

Jasechko, S., Birks, S. J., Gleeson, T., Wada, Y., Fawcett, P. J., Sharp, Z. D., et al. (2014). The pronounced seasonality of global groundwater recharge. *Water Resources Research*, *50*(11), 8845–8867. https://doi.org/10.1002/2014WR015809

Ji, S., Nie, J., Lechler, A., Huntington, K. W., Heitmann, E. O., & Breecker, D. O. (2018). A symmetrical CO2 peak and asymmetrical climate change during the middle Miocene. *Earth and Planetary Science Letters*, *499*, 134–144. https://doi.org/10.1016/j.epsl.2018.07.011

Kabeya, N., Katsuyama, M., Kawasaki, M., Ohte, N., & Sugimoto, A. (2007). Estimation of mean residence times of subsurface waters using seasonal variation in deuterium excess in a small headwater catchment in Japan. *Hydrological Processes*, *21*(3), 308–322. https://doi.org/10.1002/hyp.6231

Kelson, J. R., Huntington, K. W., Breecker, D. O., Burgener, L. K., Gallagher, T. M., Hoke, G. D., & Petersen, S. V. (2020). A proxy for all seasons? A synthesis of clumped isotope data from Holocene soil carbonates. *Quaternary Science Reviews*, *234*, 106259. https://doi.org/10.1016/j.quascirev.2020.106259

Kelson, J. R., Huth, T. E., Passey, B. H., Levin, N. E., Petersen, S. V., Ballato, P., et al. (2023). Triple oxygen isotope compositions of globally distributed soil carbonates record widespread evaporation of soil waters. *Geochimica et Cosmochimica Acta*, *355*, 138–160. https://doi.org/10.1016/j.gca.2023.06.034

Kim, S.-T., & O'Neil, J. R. (1997). Equilibrium and nonequilibrium oxygen isotope effects in synthetic carbonates. *Geochimica et Cosmochimica Acta*, *61*(16), 3461–3475. https://doi.org/10.1016/S0016-7037(97)00169-5

La Follette, P., Ogden, F. L., & Jan, A. (2023). Layered green and Ampt infiltration with redistribution. *Water Resources Research*, *59*(7), e2022WR033742. https://doi.org/10.1029/2022WR033742

Levin, N. E., Brown, F. H., Behrensmeyer, A. K., Bobe, R., & Cerling, T. E. (2011). Paleosol carbonates from the Omo Group: Isotopic records of local and regional environmental change in East Africa. *Palaeogeography, Palaeoclimatology, Palaeoecology*, *307*(1–4), 75–89. https://doi.org/10.1016/j.palaeo.2011.04.026

Liu, Z., Yoshimura, K., Bowen, G. J., Buenning, N. H., Risi, C., Welker, J. M., & Yuan, F. (2014). Paired oxygen isotope records reveal modern North American atmospheric dynamics during the Holocene. *Nature Communications*, *5*(1), 3701. https://doi.org/10.1038/ncomms4701

Montañez, I. P. (2013). Modern soil system constraints on reconstructing deep-time atmospheric CO2. *Geochimica et Cosmochimica Acta*, *101*, 57–75. https://doi.org/10.1016/j.gca.2012.10.012

Oerter, E. J., & Amundson, R. (2016). Climate controls on spatial temporal variations in the formation of pedogenic carbonate in the western Great Basin of North Americ. *Bulletin of the Geological Society of America*, *128*(7), 1095–1104. https://doi.org/10.1130/B31367.1

Oerter, E. J., & Bowen, G. J. (2017). In situ monitoring of H and O stable isotopes in soil water reveals ecohydrologic dynamics in managed soil systems. *Ecohydrology*, *10*(4), 1–13. https://doi.org/10.1002/eco.1841

Oerter, E. J., & Bowen, G. J. (2019). Spatio-temporal heterogeneity in soil water stable isotopic composition and its ecohydrologic implications in semiarid ecosystems. *Hydrological Processes*, *33*(March), 1–1738. https://doi.org/10.1002/hyp.13434

Orlowski, N., Kraft, P., & Breuer, L. (2015). Exploring water cycle dynamics through sampling multitude stable water isotope pools in a small developed landscape of Germany. https://doi.org/10.5194/hessd-12-1809-2015

Passey, B. H. (2012). Reconstructing terrestrial environments using stable isotopes in fossil teeth and paleosol carbonates. *Reconstructing Earth's Deep-Time Climate*, *18*, 167–194. https://doi.org/10.1017/S1089332600002606

Passey, B. H., Hu, H., Ji, H., Montanari, S., Li, S., Henkes, G. A., & Levin, N. E. (2014). Triple oxygen isotopes in biogenic and sedimentary carbonates. *Geochimica et Cosmochimica Acta*, *141*, 1–25. https://doi.org/10.1016/J.GCA.2014.06.006

Peters, N. A., Huntington, K. W., & Hoke, G. D. (2013). Hot or not? Impact of seasonally variable soil carbonate formation on paleotemperature and O-isotope records from clumped isotope thermometry. *Earth and Planetary Science Letters*, *361*, 208–218. https://doi.org/10.1016/j.epsl.2012.10.024

Prud'homme, C., Lécuyer, C., Antoine, P., Hatté, C., Moine, O., Fourel, F., et al. (2018). δ 13 C signal of earthworm calcite granules: A new proxy for palaeoprecipitation reconstructions during the last glacial in western Europe. *Quaternary Science Reviews*, *179*, 158–166. https://doi.org/10.1016/j.quascirev.2017.11.017

Quade, J., Garzione, C., & Eiler, J. (2007). Paleoelevation reconstruction using pedogenic carbonates. *Reviews in Mineralogy and Geochemistry*, *66*(1), 53–87. https://doi.org/10.2138/rmg.2007.66.3

Quade, M., Brüggemann, N., Graf, A., Vanderborght, J., Vereecken, H., & Rothfuss, Y. (2018). Investigation of kinetic isotopic fractionation of water during Bare soil evaporation. *Water Resources Research*, *54*(9), 6909–6928. https://doi.org/10.1029/2018WR023159

Rothfuss, Y., Vereecken, H., & Brüggemann, N. (2013). Monitoring water stable isotopic composition in soils using gas-permeable tubing and infrared laser absorption spectroscopy. *Water Resources Research*, *49*(6), 3747–3755. https://doi.org/10.1002/wrcr.20311

Routson, C. C., McKay, N. P., Kaufman, D. S., Erb, M. P., Goosse, H., Shuman, B. N., et al. (2019). Mid-latitude net precipitation decreased with Arctic warming during the Holocene. *Nature*, *568*(7750), 83–87. https://doi.org/10.1038/s41586-019-1060-3

Rugenstein, J. K. C., & Chamberlain, C. P. (2018). The evolution of hydroclimate in Asia over the Cenozoic: A stable-isotope perspective. *Earth-Science Reviews*, *185*(May), 1129–1156. https://doi.org/10.1016/j.earscirev.2018.09.003

Salazar-Jaramillo, S., Śliwiński, M. G., Hertwig, A. T., Garzón, C. C., Gómez, C. F., Bonilla, G. E., & Guerrero, J. (2022). Changes in rainfall seasonality inferred from weathering and pedogenic trends in mid-Miocene paleosols of La Tatacoa, Colombia. *Global and Planetary Change*, *208*, 103711. https://doi.org/10.1016/j.gloplacha.2021.103711

Scholl, M. A., Ingebritsen, S. E., Janik, C. J., & Kauahikaua, J. P. (1996). Use of precipitation and groundwater isotopes to interpret regional hydrology on a tropical volcanic island: Kilauea volcano area, Hawaii. *Water Resources Research*, *32*(12), 3525–3537. https://doi.org/10.1029/95WR02837

Seeger, S., & Weiler, M. (2021). Temporal dynamics of tree xylem water isotopes: In situ monitoring and modeling. *Biogeosciences*, *18*(15), 4603–4627. https://doi.org/10.5194/bg-18-4603-2021

Shuman, B. N., & Marsicek, J. (2016). The structure of Holocene climate change in mid-latitude North America. *Quaternary Science Reviews*, *141*, 38–51. https://doi.org/10.1016/j.quascirev.2016.03.009

Shuman, B. N., & Serravezza, M. (2017). Patterns of hydroclimatic change in the Rocky Mountains and surrounding regions since the last glacial maximum. *Quaternary Science Reviews*, *173*, 58–77. https://doi.org/10.1016/j.quascirev.2017.08.012

Snell, K. E., Thrasher, B. L., Eiler, J. M., Koch, P. L., Sloan, L. C., & Tabor, N. J. (2013). Hot summers in the Bighorn basin during the early Paleogene. *Geology*, *41*(1), 55–58. https://doi.org/10.1130/G33567.1

Sprenger, M., Leistert, H., Gimbei, G., & Weiler, M. (2016). Illuminating hydrological processes at the soil-vegetation-atmosphere interface with water stable isotopes. *Reviews of Geophysics*, *54*, 674–704. https://doi.org/10.1002/2015rg000515

Sprenger, M., Seeger, S., Blume, T., & Weiler, M. (2016). Travel times in the vadose zone: Variability in space and time. *Water Resources Research*, *52*(8), 5727–5754. https://doi.org/10.1002/2015WR018077

Steen-Larsen, H. C., & Zannoni, D. (2024). A versatile water vapor generation module for vapor isotope calibration and liquid isotope measurements. *Atmospheric Measurement Techniques*, *17*(14), 4391–4409. https://doi.org/10.5194/amt-17-4391-2024

Steig, E. J. (1999). Mid-Holocene climate change. *Science*, *286*(5444), 1485–1487. https://doi.org/10.1126/science.286.5444.1485

Stern, L. a., Baisden, W. T., & Amundson, R. (1999). Processes controlling the oxygen isotope ratio of soil CO2: Analytic and numerical modeling. *Geochimica et Cosmochimica Acta*, *63*(6), 799–814. https://doi.org/10.1016/S0016-7037(98)00293-2

Tripati, A. K., Hill, P. S., Eagle, R. A., Mosenfelder, J. L., Tang, J., Schauble, E. A., et al. (2015). Beyond temperature: Clumped isotope signatures in dissolved inorganic carbon species and the influence of solution chemistry on carbonate mineral composition. *Geochimica et Cosmochimica Acta*, *166*, 344–371. https://doi.org/10.1016/j.gca.2015.06.021

Winnick, M. J., Caves, J. K., & Chamberlain, C. P. (2015). A mechanistic analysis of early Eocene latitudinal gradients of isotopes in precipitation. *Geophysical Research Letters*, *42*(19), 8216–8224. https://doi.org/10.1002/2015GL064829

Zamanian, K., Pustovoytov, K., & Kuzyakov, Y. (2016). Pedogenic carbonates: Forms and formation processes. *Earth-Science Reviews*, *157*, 1–17. https://doi.org/10.1016/j.earscirev.2016.03.003

Zhang, L., Wang, C., Wignall, P. B., Kluge, T., Wan, X., Wang, Q., & Gao, Y. (2018). Deccan volcanism caused coupled *p* CO2 and terrestrial temperature rises, and pre-impact extinctions in northern China. *Geology*, *46*(3), 271–274. https://doi.org/10.1130/G39992.1

References From the Supporting Information

Kopf, S., Davidheiser-Kroll, B., & Kocken, I. (2021). Isoreader: An R package to read stable isotope data files for reproducible research. *Journal of Open Source Software*, *6*(61), 2878. https://doi.org/10.21105/joss.02878

Pagel, M. (2000). *Cathodoluminescence in geosciences*. Springer.

Stuiver, M., & Polach, H. A. (1977). Discussion reporting of ^{14}C data. *Radiocarbon*, *19*(3), 355–363. https://doi.org/10.1017/S0033822200003672